DOI: 10.1002/cmdc.200800256

Hemisuccinate of 21-Hydroxy-6,19-Epoxyprogesterone: A Tissue-Specific Modulator of the Glucocorticoid Receptor

Lautaro D. Álvarez,[a] Marcelo A. Martí,[b, c] Adriana S. Veleiro,[a] Rosana I. Misico,[a] Darío A. Estrin,[b] Adalí Pecci,[c] and Gerardo Burton*[a]

The introduction of a hemisuccinate group at the 21-position of the passive antiglucocorticoid 21OH-6,19OP leads to a compound (21HS-6,19OP) with a notable activity profile toward the glucocorticoid receptor (GR). In contrast to the parent steroid, 21HS-6,19OP behaves as a pure agonist of GR activity in direct transactivation assays. However, the apoptotic effects of 21HS-6,19OP show that the effect depends on cell type: while 21HS-6,19OP is a pure agonist in L929 mouse fibroblasts, in thymocytes 21HS-6,19OP had significant antiglucocorticoid activity. This tissue-specific activity makes 21HS-6,19OP a novel selective GR modulator. To investigate the molecular basis of action of 21HS-6,19OP, we carried out molecular dynamics simulations (6 ns) of the GR ligand binding domain (LBD) complexed with 21HS-6,19OP. Our results indicate that the hemisuccinate moiety may play a key role in stabilizing the active conformation of the receptor dimerization interface, reverting the changes observed with the antagonist 21OH-6,19OP. Other changes in regions of the GR related to cofactor recruitment (possibly tissue-specific), could explain this particular activity profile.

Introduction

Glucocorticoids exert profound and diverse physiological effects on a wide range of cell types. They participate in numerous processes such as glucose homeostasis, the metabolism of proteins, lipids and carbohydrates, as well as development and neurobiology.[1,2] In addition, glucocorticoids are potent cell-type-specific immunosuppressive and anti-inflammatory agents that work largely through the interruption of cytokine-mediated pathways. These effects are also complemented by the ability of glucocorticoids to regulate the programmed cell death of many cells. Thus, glucocorticoids induce apoptosis in most nucleated cells of the vascular system such as thymocytes, myeloma cells, and blood monocytes. In contrast, they play an anti-apoptotic role in cells, tissues, and organs in which inflammation takes place, such as mammary gland, hepatocytes, and fibroblasts.[3] As a class of pharmacological drugs, glucocorticoids are among the most widely prescribed in the world for the treatment of immune and inflammatory diseases including asthma, rheumatoid arthritis, ulcerative colitis, and allergic rhinitis.[2] They are also a component of many chemotherapeutic treatments for leukemias, lymphomas, and myelomas because of their role in the induction of apoptosis.[4,5] However, long-term use of glucocorticoids has been limited by adverse side effects ranging from suppression of the hypothalamic–pituitary axis and growth retardation, to osteoporosis, in addition to the development of glucocorticoid resistance.[5]

Glucocorticoids exert their effects by binding to the glucocorticoid receptor (GR), a transcription factor capable of regulating several genes in a positive or negative way.[2,6] The GR is a member of the family of steroid receptors (SR), which belong to the superfamily of nuclear receptors (NR).[7,8] Like most of the NR, the GR is a modular protein that is organized into three major domains: an N-terminal activation function-1 (AF-1) domain containing a ligand-independent transcriptional activation function; a central DNA binding domain (DBD) that recognizes specific sequences termed glucocorticoid response elements (GREs) in target gene promoters; a dimerization region and a C-terminal ligand binding domain (LBD), which, in addition to the ligand binding pocket (LBP), contains two fundamental regions: a second dimerization interface and an activation domain (AF-2) involved in the recognition of co-repressors and co-activators.[9,10]

In the absence of hormone, the GR resides in the cytoplasm as a multiprotein complex composed of chaperones and immunophilins. After binding of the ligand to the GR, a conformational change results in dissociation of the complex and translocation to the nucleus. Once in the nucleus, the GR modulates gene expression through two main modes of action: transactivation and transrepression.[1,2] The transactivation mode involves the binding of GR homodimers to GREs located

[a] *L. D. Álvarez, Prof. A. S. Veleiro, Dr. R. I. Misico, Prof. G. Burton*
Departamento de Química Orgánica and UMYMFOR-CONICET
Facultad de Ciencias Exactas y Naturales, Universidad de Buenos Aires
Ciudad Universitaria, Pabellón 2, C1428EGA Buenos Aires (Argentina)
Fax: (+54) 11-4576-3385
E-mail: burton@qo.fcen.uba.ar

[b] *Dr. M. A. Martí, Prof. D. A. Estrin*
Departamento de Química Inorgánica
Analítica y Química Física and INQUIMAE-CONICET
Facultad de Ciencias Exactas y Naturales
Universidad de Buenos Aires (Argentina)

[c] *Dr. M. A. Martí, Prof. A. Pecci*
Departamento de Química Biológica and IFIBYNE-CONICET
Facultad de Ciencias Exactas y Naturales
Universidad de Buenos Aires (Argentina)

in the promoter region of target genes and the subsequent binding of specific co-activators to the AF-2 domain of the GR, one of the key events in initiating transcriptome assembly and gene transcription. On the other hand, the transrepression mode involves modulation of the transcriptional activity of other transcription factors such as NF-κB, AP-1, and STATs. The GR-mediated mechanism of NF-κB and AP-1 repression has yet to be fully defined; however, it is known that the GR monomer may physically interact with these factors, inhibiting their transcriptional activity.[11]

Currently, the main goal in the drug design field of the NR, and particularly the GR, is to chemically alter the ligand properties in order to appropriately modulate receptor activities. Ligands that display differential tissue effects, such as the selective estrogen receptor modulator tamoxifen, have been commonly referred to as selective NR modulators (SNuRMs).[7,8] Converging evidence has demonstrated that the mixed agonist/antagonist properties of SNuRMs are associated with the differential recruitment of tissue-specific cofactors to the receptors.[12] In the case of glucocorticoids, recent advances in the study of the molecular mechanisms of GR action, together with the determination of the tertiary structure of the GR LBD, have promoted increasing interest in the development of novel tissue-selective ligands or selective glucocorticoid receptor modulators (SGRMs) that can modulate certain GR activities to treat specific diseases.

To understand how a specific ligand modulates the conformation and dynamic behavior of its receptor, it is necessary to analyze the ligand–receptor interaction at the molecular level. Recently, to investigate the molecular basis of the passive antagonism exhibited by 21-hydroxy-6,19-epoxyprogesterone (21OH-6,19OP),[13] we performed molecular dynamics (MD) simulations on three different binding states of the GR LBD: an agonist system (GR LBD–dexamethasone [dex]), an antagonist system (GR LBD–21OH-6,19OP), and an unbound system (see Figure 1 for ligand structures).[14] Our results showed that the state of the LBP of the GR LBD determines receptor behavior during the simulation, with significant differences between the interaction hydrogen bond patterns of GR LBD–21OH-6,19OP and GR LBD–dex. These differences would explain the different evolution of fundamental regions of the receptor observed in the GR LBD–21OH-6,19OP complex. In particular, we observed that the H1–H3 loop of the GR LBD–21OH-6,19OP complex adopts an average position located significantly further away from the rest of the protein, resulting in a major conformational change in the dimerization interface relative to the GR LBD–dex complex. Taking into account that the GR–21OH-6,19OP complex is unable to induce the transactivation activity of mouse mammary tumor virus (MMTV) promoters, our findings support the hypothesis that the passive antagonism mode of action of 21OH-6,19OP involves the inability of the complex to homodimerize.

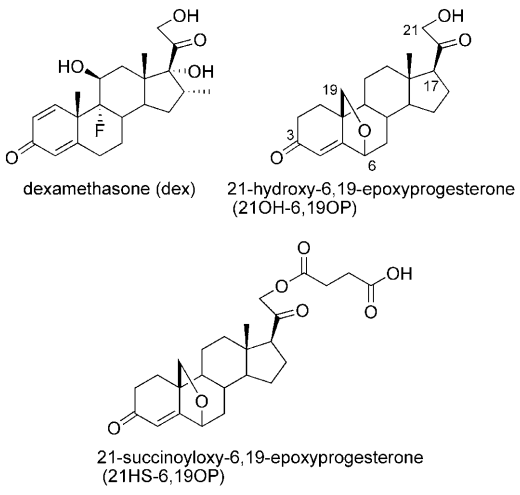

Figure 1. Structures of GR ligands.

The hemisuccinate derivative of 21OH-6,19OP (21HS-6,19OP, Figure 1) was prepared among others to improve the solubility of the parent compound in biological media. However, preliminary activity testing showed a dramatic change in the activity profile that turned 21HS-6,19OP into a potential SGRM. Herein we report our investigations of the activity of 21HS-6,19OP by a combination of experimental and computer simulation tools.

Results

Transactivation activity of 21HS-6,19OP

We started the evaluation of the biological activity of 21HS-6,19OP by testing its direct transactivation ability in Cos-1 cells, which lack endogenous steroid receptors. Cos-1 cells were co-transfected with a plasmid coding for the human glucocorticoid receptor (hGR) and the MMTV–luciferase (Luc) reporter, in which luciferase expression is driven by a promoter that contains glucocorticoid-specific response elements capable of binding to GR-activated homodimers.[15] The potent agonist dex was used as control of glucocorticoid activity. Unexpectedly, the results showed that in contrast to the parent compound 21OH-6,19OP, 21HS-6,19OP exhibits significant dose-dependent glucocorticoid activity per se, with no inhibitory effects toward dex action (i.e., no antiglucocorticoid activity) (Figure 2a).

To further characterize the transactivation activity of 21HS-6,19OP, we used the same MMTV–Luc reporter method, but in L929 cells, a cell line derived from mouse fibroblast that expresses endogenous GR. As in Cos-1 cells, the hemisuccinate derivative had glucocorticoid activity but no antiglucocorticoid activity (Figure 2b). The lower fold induction observed in the L929 assay relative to the Cos-1 assay may be attributed to less efficient plasmid transfection in the former cells and/or to the greater number of GR when the receptor is overexpressed by transient transfection. We have therefore shown that 21HS-6,19OP is able to bind both recombinant hGR and endogenous mouse GR, thus activating the translocation and dimerization of the receptor and inducing the transcription of the MMTV–Luc reporter.

To test its specificity, 21HS-6,19OP was also assayed in Cos-1 cells expressing the human progesterone receptor (PR). As is the case with 21OH-6,19OP, the hemisuccinate derivative failed to antagonize the agonist effect of R5020 or to act as an ago-

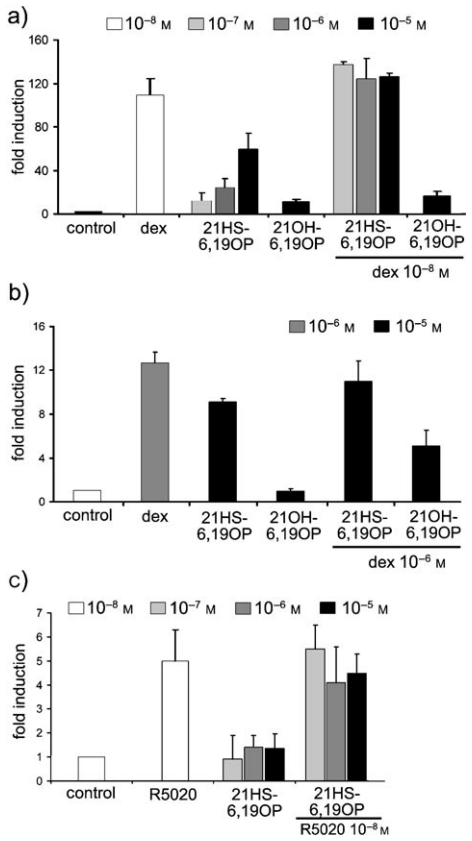

Figure 2. Transactivation activity of 21HS-6,19OP. a) Cos-1 cells were co-transfected with pRSV–hGR vector (1 μg), pMMTV–Luc reporter vector (3 μg), and pCMV–LacZ vector (1 μg). b) L929 cells were co-transfected with pMMTV–Luc reporter vector (3 μg) and pCMV–LacZ vector (1 μg). c) Cos-1 cells were co-transfected with pRSV–hPR vector (1 μg), pMMTV–Luc reporter vector (3 μg), and pCMV–LacZ vector (1 μg). In all assays, cells were incubated for 24 h as indicated, and luciferase activity was measured. After correcting for β-galactosidase activity, the values are expressed as fold induction relative to control (untreated cells). Data represent the mean ± SE from three independent experiments.

nist per se at all concentrations tested (Figure 2c). These results indicate that GR/PR selectivity is conserved when the hemisuccinate group is added to the 21-position of 21OH-6,19OP.

Apoptotic activity of 21HS-6,19OP in L929 cells

The protective role of glucocorticoid agonists in the TNF-α-mediated cytotoxic effect on mouse fibroblast L929 cells is a well-characterized model to evaluate the apoptotic/anti-apoptotic activity of novel ligands.[16] We used this model to further determine the glucocorticoid/antiglucocorticoid activity of the novel ligand 21HS-6,19OP. Figure 3 shows that after treatment with TNF-α at 1 ng mL^{-1} for 24 h, the cell viability decreased to 54%. Cell survival increased to 88% when cells were co-treated with dex at 10^{-5} M, indicating the protective role of dex in TNF-α-induced apoptosis. Both 21HS-6,19OP and 21OH-6,19OP exhibited significant glucocorticoid activity, with 83 and 73% cell survival, respectively. When cells were treated with dex plus 21HS-6,19OP or 21OH-6,19OP, cell survival was 90 and

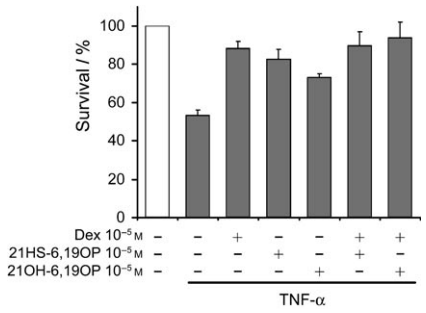

Figure 3. Apoptotic activity of 21HS-6,19OP in L929 cells. L929 cells were stimulated with TNF-α (1 ng mL^{-1}) in the presence or absence of the various steroids as indicated for 24 h. Cell viability was then assessed by crystal violet staining assays. Percentage of survival is shown relative to control (untreated cells). Data represent the mean ± SE from three independent experiments.

94%, respectively, indicating that both rigid analogues do not have antiglucocorticoid action.

Apoptotic activity of 21HS-6,19OP in mouse thymocytes

Apoptosis of thymocytes has been repeatedly used as a representative parameter of glucocorticoid-mediated immunosuppression.[17,18] In these cells, glucocorticoid agonists such as dex have pro-apoptotic or immunosuppressive effects. Thus, immunosuppressive and anti-immunosuppressive activities of 21HS-6,19OP were evaluated by the ability of this compound to induce apoptosis in thymocyte primary culture or to block this dexamethasone-mediated effect. Apoptosis was determined by using the annexin method described previously.[19] Figure 4 shows that dex (at 10^{-8} M) increased apoptosis two-fold, while 21HS-6,19OP increased apoptosis ~1.4-fold at all concentrations assayed.

In contrast, the parent compound 21OH-6,19OP did not present an immunosuppressive effect per se. Remarkably, when we evaluated the capacity of 21HS-6,19OP as an antiglucocorticoid, we found that it efficiently blocked the apoptotic

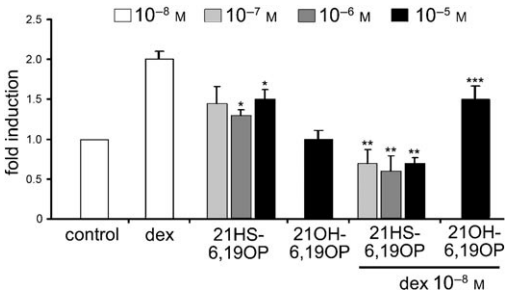

Figure 4. Apoptotic activity of 21HS-6,19OP in mouse thymocytes. Thymocytes were incubated as indicated for 4 h. A fluorescein isothiocyanate (FITC) conjugate of annexin V was used to detect apoptosis by flow cytometry. Positive annexin V cells were analyzed as described previously. Results are expressed as the mean fold induction relative to control (untreated cells). Data represent the mean ± SE from three independent experiments; *$p < 0.05$ vs. control, **$p < 0.01$ vs. dex, ***$p < 0.05$ vs. dex. Induction of apoptosis by dex (10^{-8} M) + 21HS-6,19OP (10^{-8} M) did not differ significantly from dex alone (10^{-8} M; data not shown).

dexamethasone-mediated effect at all concentrations assayed. The anti-immunosuppressive effect of 21HS-6,19OP was so strong that even the untreated cells (control) had a higher apoptotic level than the cells treated with dex plus 21HS-6,19OP. As reported previously,[20] 21OH-6,19OP also inhibits the dex effect, although to much lesser extent than 21HS-6,19OP.

Molecular dynamics simulation

To better understand the differential activity profile of the two rigid analogues, and to investigate the molecular basis of action of 21HS-6,19OP, we performed a 6-ns molecular dynamics simulation of the GR LBD–21HS-6,19OP complex. Comparison of the resulting trajectory with that previously obtained with GR LBD–dex and GR LBD–21OH-6,19OP complexes[14] showed important differences both in the ligand binding mode and in the behavior of fundamental regions of the GR LBD.

Ligand binding mode

Based on ligand binding mode analysis, we previously showed that the overall position of the steroid skeleton of 21OH-6,19OP and dex are similar.[14] Moreover, the C3 carbonyl group of 21OH-6,19OP is involved in a hydrogen bonding network similar to that observed in the dex simulation. At the other end of the molecule, and in contrast with the dex system, the 21-hydroxy group of 21OH-6,19OP does not present an alternate behavior. A hydrogen bond interaction with Asp564 is formed at the beginning of the simulation, and this interaction remains stable during the timescale of the simulation. We proposed that this differential pattern of hydrogen bonding of Asn564 (located within helix 3) influences the differential evolution of the H1–H3 loop observed in the GR LBD–dex and GR LBD–21OH-6,19OP complexes.

To perform the MD simulation of the GR LBD–21HS-6,19OP complex, 21HS-6,19OP was introduced superimposing the carbon atoms of the C ring with the corresponding carbon atoms of dex. 21HS-6,19OP has the same carbon skeleton as 21OH-6,19OP, but instead of the hydroxy group at position 21, it has the bulky polar side chain of the hemisuccinate substituent. The hemisuccinate moiety is located within the open cavity of the receptor formed by helices H3, H11, and H7 in a manner that minimizes steric hindrance. Visual inspection of the trajectory of the GR LBD–21HS-6,19OP complex shows that both the overall position and conformation of the steroid skeleton are very similar to those adopted by 21OH-6,19OP in the GR LBD–21OH-6,19OP complex. The hydrogen bonding network observed around the A rings of dex and 21OH-6,19OP is also present in this system. As in the 21OH-6,19OP system, there is no interaction between the oxygen atom of the intramolecular 6,19 bridge of 21HS-6,19OP and the polar residues of the LBP. The main difference between the two rigid steroids (21OH-6,19OP and 21HS-6,19OP) is the behavior of the side chain. In the case of 21HS-6,19OP, the hemisuccinate group remains around its initial position during the timescale of the simulation (Figure 5a). Interestingly, we found that the terminal carboxylate group of the hemisuccinate moiety forms a strong and stable interaction with the phenolic hydroxy group of Tyr735, a residue located within helix 11 that does not form part of the LBP. Analysis of the time evolution of the distances between the oxygen atoms of this carboxylate group and the oxygen atom of the Tyr735 OH group revealed that at least one hydrogen bond persists (Figure 5b). This additional stable ligand–receptor interaction might play a fundamental role in the conformational changes of the receptor, as described below.

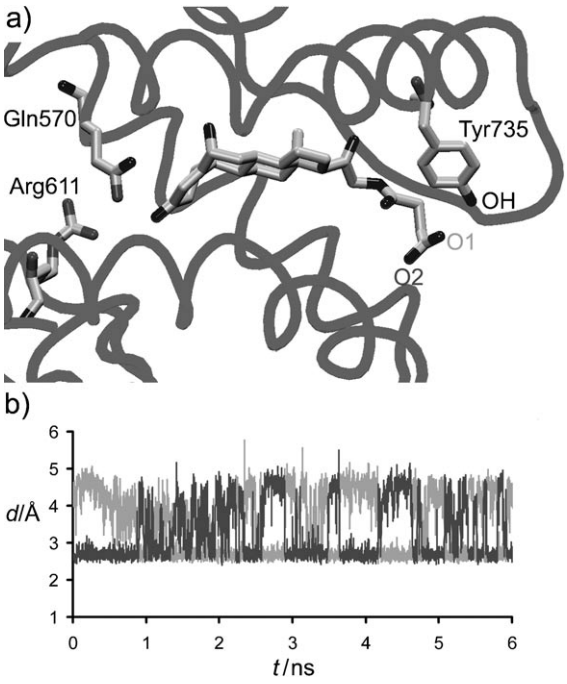

Figure 5. Ligand binding mode analysis. a) Average structure of 21HS-6,19OP within the LBP. Residues Gln570, Arg611, and Tyr735 that form hydrogen bond interactions with 21HS-6,19OP are shown. b) Time evolution of the distance (*d*) between the hydroxy oxygen atom of residue Tyr735 and ligand O1 (light gray) and O2 (dark gray) oxygen atoms. Distances < 3.5 Å indicate that strong and stable H bonds are formed.

Dimer interface

We previously proposed that the passive antagonism of 21OH-6,19OP on the transactivation activity of GR could reside in the inability of the GR–21OH-6,19OP complex to dimerize as a result of the allosteric change caused by the ligand in the H1–H3 loop conformation.[14] Thus, while the presence of the agonist dex leads to an average conformation of the receptor in which the N-terminal region of the H1–H3 loop is close to the protein body, the presence of 21OH-6,19OP in the LBP significantly alters the dynamic behavior of this dimerization region of the receptor. Besides the receptor adopting an average conformation in which the H1–H3 loop is located significantly further away from the rest of the protein, the fluctuation of this loop during the simulations is small relative to the dex system. Following these considerations, the dynamic behavior of the

H1–H3 loop of the GR LBD–21HS-6,19OP complex was evaluated both in its average position and fluctuation. Figure 6a shows that, as in the 21OH-6,19OP system, the H1–H3 loop of the GR LBD–21HS-6,19OP complex has a smaller fluctuation than the H1–H3 loop of the dex system. However, in contrast to the 21OH-6,19OP system, the average conformation of the loop is very similar to the conformation adopted by the H1–H3 loop in the GR LBD–dex complex (Figure 6b). Visual inspection of the GR LBD–-21HS-6,19OP trajectory reveals that upon an initial period in which the H1–H3 loop has a high fluctuation, caused by the presence of the bulky hemisuccinate group, the loop looses mobility and adopts a position close to the protein body, very similar to the position adopted by the loop in the dex system and significantly different from the H1–H3 loop position of the 21OH-6,19OP system.

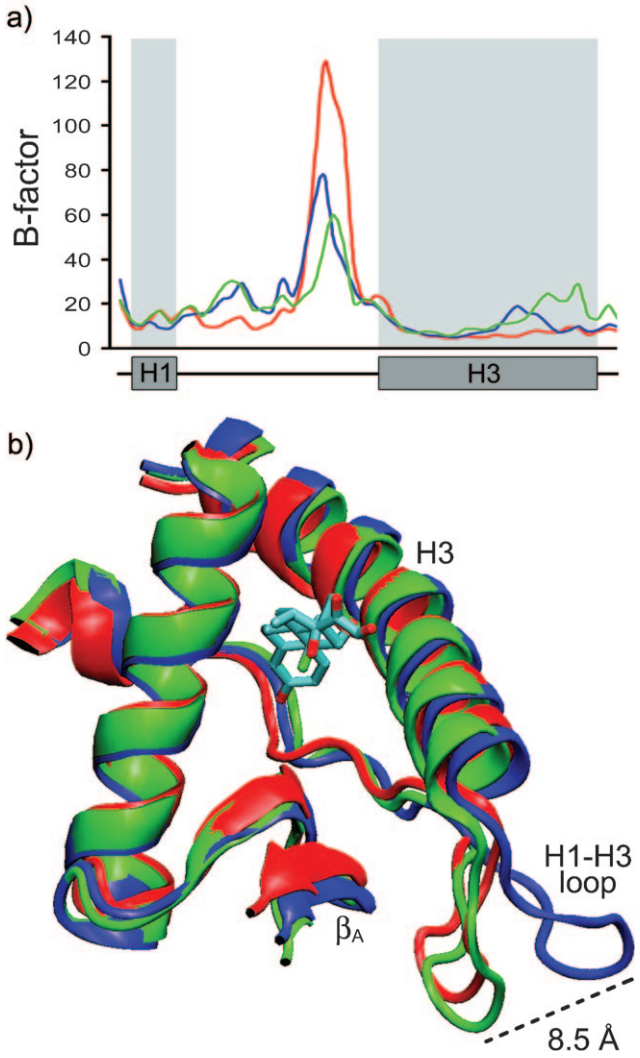

Figure 6. Dimer interface analysis. a) Comparison of B-factors of the H1–H3 loop of the three systems over the last 4 ns of MD simulation (GR LBD–dex in red; GR LBD–21OH-6,19OP in blue, and GR LBD–21HS-6,19OP in green). The secondary structure of GR LBD is schematized along the *x*-axis: H1 is formed by residues 533–539, and H3 is formed by residues 556–579. b) Average structure of the H1–H3 loop in the three systems (GR LBD–dex in red; GR LBD–21OH-6,19OP in blue, and GR LBD–21HS-6,19OP in green) taken over the last 4 ns of MD simulation. The ligand shown is dexamethasone in the GR LBD–dex complex.

AF-2 domain

The AF-2 conformation of GR LBD is mainly determined by the position of the dynamic helix 12. We have shown previously that the average conformation of H12 is slightly altered by the presence of 21OH-6,19OP in the LBP, resulting in a decrease in the dimension of the AF-2 domain of the GR LBD–21OH-6,19OP complex relative to the GR LBD–dex complex.[14] In addition to this subtle change, a major change was observed in the behavior of residues 762–767. These residues, originally located in a loop region contiguous to H12, adopt a more structured conformation, making H12 longer by five residues in the 21OH-6,19OP system with respect to the original system.

To investigate the influences of 21HS-6,19OP in the conformation of H12, the average conformation was obtained and superimposed with that previously obtained for the GR LBD–dex and GR LBD–21OH-6,19OP complexes. As with the 21OH-6,19OP system, the 21HS-6,19OP system also induced residues 762–767 to acquire a helix motif (Figure 7a). However, the

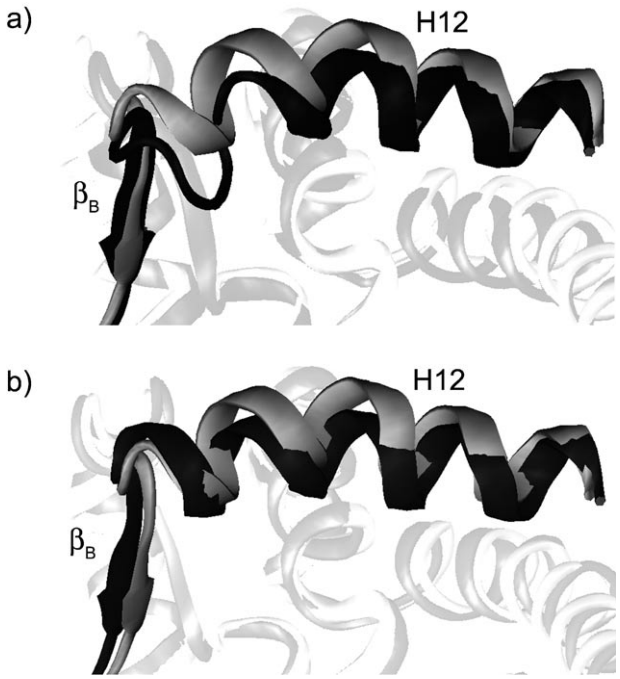

Figure 7. H12 conformation analysis. H12 average structure of a) GR LBD–dex (dark gray) and GR LBD–21HS-6,19OP (light gray), and b) GR LBD–21HS-6,19OP (light gray) and GR LBD–21OH-6,19OP (dark gray) taken over the last 4 ns of MD simulation (data for GR LBD–dex and GR LBD–21OH-619OP complexes taken from ref. [14]).

presence of the bulky hemisuccinate group induced a significant displacement of the average position of H12 in the GR LBD–21HS-6,19OP complex with respect to the H12 position in both GR LBD–dex and GR LBD–21OH-6,19OP complexes. This modification of the H12 conformation produced changes in the overall conformation of the AF-2 domain of the GR LBD–21HS-6,19OP complex relative to the dex system, possibly altering the cofactor binding ability.

Discussion

One point for initial consideration is the stability of the hemisuccinate moiety in biological media. Two pieces of evidence support the integrity of 21HS-6,19OP throughout the experiments. First, the significant differences observed after 24 h in Cos-1 cells between 21HS-6,19OP and 21OH-6,19OP indicate that no ester hydrolysis had occurred. Second, other esters (acetate, propionate, oleate) were inactive in the thymocyte apoptosis assay, indicating that ester hydrolysis did not occur under the experimental conditions used (data not shown). 21HS-6,19OP was also stable when incubated at 10^{-3} M in RPMI 1640 (half-life: 72 h).

Transactivation activity

The opposite results observed between 21OH-6,19OP and 21HS-6,19OP in the direct transactivation assay (Figure 2) revealed that the hemisuccinate group plays a key role in the ligand–receptor interaction, stabilizing the GR–21HS-6,19OP complex in an active conformation that is able to induce the transcription of the MMTV–Luc reporter. To investigate this fact at the molecular level, we used MD simulations, a computational technique that takes protein flexibility into consideration in the ligand–receptor interaction. This is necessary for investigating how the ligands modulate the receptor structure. Our MD simulation showed that within the GR LBD there is a cavity formed by H11, H7, and H3 in which the hemisuccinate group of 21HS-6,19OP may be accommodated without steric hindrance. Moreover, ligand binding mode analysis revealed the presence of a strong interaction between the terminal carboxylate group of 21HS-6,19OP and Tyr735 (Figure 5). Somehow, the presence of the hemisuccinate group in this cavity, together with this stable ligand–receptor interaction, causes the average conformation of the H1–H3 loop of the GR LBD–21HS-6,19OP complex to mimic that found in the GR LBD–dex complex and to differ from that in the GR LBD–21OH-6,19OP complex (Figure 6). As this loop is a fundamental part of the dimerization interface, and the transactivation activity of glucocorticoids requires the binding of GR homodimers to the GRE, the simulation results suggest that the switch of antagonism to agonism observed upon the attachment of a hemisuccinate group at position 21 of 21OH-6,19OP could be explained by considering that this group stabilizes a H1–H3 loop conformation that facilitates homodimerization. In this way, although both rigid analogues bind to GR and induce the translocation of the complex, the GR–21OH-6,19OP complex would be unable to homodimerize, while the GR–21HS-6,19OP complex may indeed homodimerize and thus activate gene transcription. Recent X-ray crystallographic studies of the GR LBD–deacylcortivazol complex demonstrated that the GR can expand the LBP to accommodate large groups protruding from the A ring in a cavity involving H3, H4, and H5 without significant distortions to its overall conformation.[21] According to the MD results, this could be another striking example of GR adaptability in which the LBP would extend to the cavity formed by H11, H7, and H3.

Although the lower transactivation potency of 21HS-6,19OP relative to dex (Figure 2) can be explained assuming a lower affinity of 21HS-6,19OP for binding to GR, another explanation is possible based on the co-activator/co-repressor equilibrium model for GR-mediated activation or repression of gene transcription.[22,23] It has been demonstrated that the transcriptional potency of a steroid receptor ligand is sensitive not only to ligand concentration, but to the concentration of receptor, cofactors, and DNA. Upon binding to the SR, the co-activators recruit histone acetyl transferases, which remodel the chromatin, inducing gene transcription.[24] In contrast, co-repressors binding to the SR result in a recruitment of histone deacetylases, leading to transcription repression.[25] Like the rest of SRs, both activating and repressing cofactors of GR use a similar or overlapping binding groove on the LBD.[26] The model mentioned above states that both agonist- and antagonist-bound GR can interact with co-activators as well as co-repressors, and that the ratio of the two populations dictates the transcriptional level. According to the MD simulation, the presence of 21HS-6,19OP within the LBP and, in particular, the presence of the bulky hemisuccinate group within the cavity formed by H3, H7, and H11 would affect the conformation of H12 (Figure 7). Consequently, we may speculate that the AF-2 domain of GR LBD–21HS-6,19OP would differ from the AF-2 domain of the GR–dex complex. This subtle modification on the surface at which the cofactors must be docked could cause an increase in the equilibrium constant of the receptor–co-repressor interaction, and/or a decrease in the equilibrium constant of the receptor–co-activator interaction, leading to a decrease in the number of active GR–21HS-6,19OP–co-activator complexes, and hence of the transcriptional potency of 21HS-6,19OP.

Apoptotic activity

Given the relevant and diverse role of glucocorticoids in the apoptotic process of several cell types, two opposite models were chosen to evaluate the apoptotic properties of 21HS-6,19OP. In the first (L929 fibroblast), glucocorticoids have an anti-apoptotic effect, whereas in the second (thymocytes), they induce apoptosis.

The protective role of dex on TNF-α-induced apoptosis in L929 cells has been widely studied, although no conclusive information has been found for the molecular mechanism involved in the action of the GR–dex complex. According to Mendoza-Milla et al., NF-κB activation is required for dex-dependent protection.[16] However, it has also been demonstrated that transrepression of NF-κB is not required for these dex effects,[27] indicating that the anti-apoptotic effects of glucocorticoids in L929 cells involve a more complex mechanism of action than the classical NF-κB transrepression mode. The apoptotic genes expressed in this response and how they are regulated by the GR–dex complex remain unknown. In this context, the molecular determinants of the action of the rigid analogues cannot be fully understood. However, considering the MD simulation results and because both rigid analogues show glucocorticoid activity (Figure 3), a mechanism in which the GR complexes act as monomers may be feasible. Interest-

ingly, it has been shown that the ability of the GR to function as co-activator in the positive regulation of genes controlled by STAT5, for example, is not affected by the dimerization and DNA binding properties of the receptor.[28] Thus, in L929 cells, the anti-apoptotic activity of 21HS-6,19OP and 21OH-6,19OP would be provided by the regulatory action of GR–21OH-6,19OP or GR–21HS-6,19OP monomers on the expression of apoptotic genes controlled by NF-κB. Importantly, while some transactivation function of the GR may be deleted to prevent GR homodimerization by a point mutation, there are clearly some genes that are positively regulated by the GR that are not affected by this mutation.[29]

The glucocorticoid role in thymocyte apoptosis is better understood. Glucocorticoids trigger thymocyte cell death mainly by modulating the expression of some members of the Bcl-2 family of proteins.[30,31] The current model implies that glucocorticoid-induced apoptosis of thymocytes requires the presence of a functional GR and, in particular, its transactivating function.[32] Reichardt et al. have shown that a mutant known as $GR^{dim/dim}$, which fails to homodimerize, conserves the NF-κB and AP-1 transrepression activities, but is unable to mediate transcription from GREs.[33] Thus, in thymocytes expressing $GR^{dim/dim}$, the glucocorticoids loose their pro-apoptotic effects.[33] We have shown that 21OH-6,19OP acts as a pure antagonist, blocking the apoptotic activity of dex and lacking effects per se (Figure 4). This experimental result correlates well with the MD simulation results, as it suggests that the GR–21OH-6,19OP monomer cannot correctly homodimerize and, as a consequence, the complex is unable to regulate transcription of the genes involved in apoptotic signaling.

The effects of 21HS-6,19OP in these assays are more complex (Figure 4). On one hand, in the presence of 21HS-6,19OP alone, it behaved as an agonist of GR, an expected result in view of the transactivation activity shown in both Cos-1 and L929 cells. On the other hand, 21HS-6,19OP in combination with dex showed a very potent antagonistic effect on dex action. Further experimental studies of the molecular mechanism of action of dex and 21HS-6,19OP in thymocytes are required to explain this phenomenon at the molecular level. However, a cofactor equilibrium model could help us understand the molecular determinants of this potent antagonism. Variation in affinity between GR–21HS-6,19OP and GR–dex complexes toward limiting and specific thymocyte cofactors could explain the results obtained. It is important to note that perhaps other non-genomic mechanisms of action of GR are involved in the global apoptotic effects of 21HS-6,19OP. Finally, improved cell penetration due to the hemisuccinate moiety cannot be ruled out, and this could explain the observed activities at lower concentrations relative to 21OH-6,19OP.

In summary, the introduction of a hemisuccinate group at the 21-position of the antiglucocorticoid 21OH-6,19OP led to a derivative with new and interesting properties. In the direct transactivation assay, 21HS-6,19OP behaved as a pure agonist of GR action. By studying the apoptotic effects of this analogue, we found that while in the L929 cells 21HS-6,19OP is a pure anti-apoptotic agonist, the apoptotic activity in thymocytes depends strongly on the presence or absence of dex in the medium. Further studies to investigate GR-dependent cofactor recruitment using 21HS-6,19OP might help improve our understanding of the tissue-specific fine-tuning of gene expression regulated by the GR. An understanding of the molecular basis for this tissue specificity is critical for the development of therapeutics with the desired agonist/antagonist profile. Lastly, the MD simulation provided valuable information that may help in understanding the complex molecular mechanisms underlying ligand–GR interactions and their effects on GR activity.

Experimental Section

Biological activity

Steroids. 21-Hydroxy-6,19-epoxyprogesterone and 21-succinoyloxy-6,19-epoxyprogesterone were prepared as described previously.[34] Dexamethasone and R5020 were purchased from Sigma (St. Louis, MO, USA).

Transactivation activity. Cos-1 and L929 cells were cultured at 37 °C under humidified atmosphere with 5% CO_2 in DMEM supplemented with 10% fetal calf serum (FCS) containing penicillin (100 IU mL^{-1}), streptomycin (100 mg mL^{-1}), and glutamine (2 mM) in p100 plates. For transient transfections, 5×10^5 cells were plated in 60-mm plates and transfected by the lipofectin method according to the manufacturer's protocol (Lipofectine Plus, Gibco, Inc.). In Cos-1 cells, analyses of the GR activity were performed by transfecting 3 μg of pMMTV–Luc plasmid, which expresses luciferase under the control of the mouse mammary tumor virus (MMTV) promoter containing several hormone-response elements, 1 μg pRSV–GR expressing the human glucocorticoid receptor,[35] and 3 μg of pRSV–LacZ (Clontech Inc., Palo Alto, CA, USA) as transfection control. In L929 cells, analyses of the GR activity were performed by transfecting 3 μg of pMMTV–Luc and 3 μg of pRSV–LacZ. In Cos-1 cells, analyses of the PR activity were performed by transfecting 3 μg of pMMTV–Luc, 1 μg pRSV–PR expressing the human progesterone receptor, and 3 μg of pRSV–LacZ. Eighteen hours after transfection, the medium was replaced by fresh medium containing 10% charcoal-stripped FCS and antibiotics. Cells were then incubated for 24 h with dexamethasone (for GR) or R5020 (for PR) with or without 21HS-6,19OP at the concentrations indicated. Steroids were applied from 1000× stock solutions in DMSO. Incubations were stopped by aspirating the medium and washing the cells twice with phosphate-buffered saline (PBS). Cells were then harvested in lysis buffer, and luciferase activity was measured according to the manufacturer's protocol (Promega Inc.). Galactosidase activity was measured as previously described.[20]

Apoptosis of L929 cells. Cell viability of L929 cells was evaluated by crystal violet staining.[36] L929 cells were plated at 3×10^5 cells per well in 96-well microtiter plates, cultured for 24 h, and then treated as indicated with TNF-α from Sigma (St. Louis, MO, USA) with or without steroids. After 24 h the cells were fixed with 100 μL ice-cold glutaraldehyde (1.1% in PBS) for 15 min at 0 °C. The plates were washed three times by submersion in de-ionized water, air-dried, and stained for 20 min with 100 μL of a 0.1% solution of crystal violet (dissolved in 200 mM phosphoric acid buffer at pH 6). After careful aspiration of the crystal violet, extensive washing with de-ionized water removed excess dye. The plates were air-dried prior to solubilization of the bound dye with 100 μL of a solution of 10% acetic acid and incubation for 30 min. The optical density of dissolved crystal violet was measured at 590 nm

with a multi-plate spectrophotometer (Benchmark, Bio-Rad, Hercules, CA, USA).

Apoptosis of thymocytes. Thymocytes were obtained from CF-1 21-day-old male mice and incubated (1×10^7 cells per well) in plastic dishes in 1 mL of RPMI 1640 containing 10% charcoal-stripped FCS, concanavalin A (2 $\mu g\,mL^{-1}$), and the various steroids at the indicated concentrations. The corresponding volume of ethanol (0.1%) was added to control cells. Cells were incubated for 4 h at 37 °C in a water bath under a normal atmosphere. After incubation, the apoptosis index was determined by an annexin V–FITC apoptosis detection kit from Clontech Inc. (Palo Alto, CA, USA). Fluorescence was detected according to the RAPID protocol recommended by the manufacturer. Briefly, after incubation, cells were centrifuged at 2000 rpm for 5 min, the media was removed, and cells were resuspended in 200 μL binding buffer ($\sim1\times10^6$ cells). Propidium iodide (5 μL) and annexin V–FITC (10 μL) were added, and cells were incubated for 15 min at room temperature in the dark. Samples were analyzed by flow cytometry in a Cytoron Absolute cytometer (Ortho Diagnostic Systems). Data were analyzed with Wimdi 2.7 software.

Computational methods

Quantum mechanics calculations. The geometry of 21-succinoyloxy-6,19-epoxyprogesterone (21HS-6,19OP) was optimized using the ab initio quantum chemistry program Gaussian 03[37] and the HF/6–31G** basis set. Restraint electrostatic potential (RESP) atomic charges were calculated.

Molecular dynamics. MD simulations were performed by using the AMBER 9 software package as previously described.[38,14] Briefly, the starting structure for the simulation was taken from the crystal structure of the GR–dexamethasone complex (chain A of PDB code: 1M2Z).[39] The GR LBD–21HS-6,19OP complex was built in silico, superimposing the carbon atoms of ring C of 21HS-6,19OP with the corresponding atoms of the dex molecule in the GR–dexamethasone complex. The ligand parameters were assigned with the general AMBER force field (GAFF), and the corresponding RESP charges using the Antechamber module of AMBER. The Amber99 force field parameters were used for all residues.[40] The complex was immersed in an octahedral box of TIP3P water molecules using the Leap module, giving a final system of around 27000 atoms. The system was initially optimized and then gradually heated at 300 K. Starting from this equilibrated structure, MD production runs of 6 ns were performed. All simulations were performed at 1 atm and 300 K, maintained with the Berendsen barostat and thermostat,[41] using periodic boundary conditions and the particle mesh Ewald method (grid spacing of 1 Å) for treating long-range electrostatic interactions with a uniform neutralizing plasma. The SHAKE algorithm was used to keep bonds involving H atoms at their equilibrium length, allowing us to employ a 2-fs time step for the integration of Newton's equations.

Acknowledgements

Financial support by Agencia Nacional de Promoción Científica y Tecnológica, CONICET (Argentina), and Universidad de Buenos Aires is gratefully acknowledged. L.D.A. thanks CONICET for a fellowship.

Keywords: apoptosis · glucocorticoid receptors · molecular dynamics · structure–activity relationships · tissue-specific activity

[1] S. van der Laan, O. C. Meijer, *Eur. J. Pharmacol.* **2008**, *585*, 483–491.
[2] B. M. Necela, J. A. Cidlowski, *Proc. Am. Thorac. Soc.* **2004**, *1*, 239–246.
[3] A. Amsterdam, R. Sasson, *Mol. Cell. Endocrinol.* **2002**, *189*, 1–9.
[4] C. Zhang, B. Beckermann, G. Kallifatidis, Z. Liu, W. Rittgen, L. Edler, P. Buchler, K. M. Debatin, M. W. Buchler, H. Friess, I. Herr, *Int. J. Oncol.* **2006**, *29*, 1295–1301.
[5] M. Sui, F. Chen, Z. Chen, W. Fan, *Int. J. Cancer* **2006**, *119*, 712–717.
[6] R. Newton, N. S. Holden, *Mol. Pharmacol.* **2007**, *72*, 799–809.
[7] J. T. Moore, J. L. Collins, K. H. Pearce, *ChemMedChem* **2006**, *1*, 504–523.
[8] H. Gronemeyer, J. A. Gustafsson, V. Laudet, *Nat. Rev. Drug Discovery* **2004**, *3*, 950–964.
[9] B. M. Necela, J. A. Cidlowski, *Trends Pharmacol. Sci.* **2003**, *24*, 58–61.
[10] R. Kumar, E. B. Thompson, *J. Steroid Biochem. Mol. Biol.* **2005**, *94*, 383–394.
[11] O. Kassel, P. Herrlich, *Mol. Cell. Endocrinol.* **2007**, *275*, 13–29.
[12] K. W. Nettles, G. L. Greene, *Annu. Rev. Physiol.* **2005**, *67*, 309–333.
[13] G. P. Vicent, M. C. Monteserin, A. S. Veleiro, G. Burton, C. P. Lantos, M. D. Galigniana, *Mol. Pharmacol.* **1997**, *52*, 749–753.
[14] L. D. Álvarez, M. A. Martí, A. S. Veleiro, D. M. Presman, D. A. Estrin, A. Pecci, G. Burton, *J. Med. Chem.* **2008**, *51*, 1352–1360.
[15] M. H. Beato, P. and G. Schütz, *Cell* **1995**, *83*, 851–857.
[16] C. Mendoza-Milla, C. Machuca Rodríguez, E. Córdova Alarcón, A. Estrada Bernal, E. M. Toledo-Cuevas, E. Martínez Martínez, A. Zentella Dehesa, *FEBS Lett.* **2005**, *579*, 3947–3952.
[17] A. H. Wyllie, *Nature* **1980**, *284*, 555–556.
[18] B. M. Vayssiere, S. Dupont, A. Choquart, F. Petit, T. Garcia, C. Marchandeau, H. Gronemeyer, M. Resche-Rigon, *Mol. Endocrinol.* **1997**, *11*, 1245–1255.
[19] A. W. Boersma, K. Nooter, R. G. Oostrum, G. Stoter, *Cytometry* **1996**, *24*, 123–130.
[20] A. S. Veleiro, A. Pecci, M. C. Monteserin, R. Baggio, M. T. Garland, C. P. Lantos, G. Burton, *J. Med. Chem.* **2005**, *48*, 5675–5683.
[21] K. Suino-Powell, Y. Xu, C. Zhang, Y. G. Tao, W. D. Tolbert, S. S. Simons, Jr., H. E. Xu, *Mol. Cell. Biol.* **2008**, *28*, 1915–1923.
[22] S. S. Simons, Jr., *Trends Pharmacol. Sci.* **2003**, *24*, 253–259.
[23] Q. Wang, J. A. Blackford, L. N. Song, Y. Huang, S. Cho, S. S. Simons, Jr., *Mol. Endocrinol.* **2004**, *18*, 1376–1395.
[24] J. Xu, Q. Li, *Mol. Endocrinol.* **2003**, *17*, 1681–1692.
[25] C. L. Smith, B. W. O'Malley, *Endocr. Rev.* **2004**, *25*, 45–71.
[26] V. Perissi, L. M. Staszewski, E. M. McInerney, R. Kurokawa, A. Krones, D. W. Rose, M. H. Lambert, M. V. Milburn, C. K. Glass, M. G. Rosenfeld, *Genes Dev.* **1999**, *13*, 3198–3208.
[27] M. A. Costas, L. Muller Igaz, F. Holsboer, E. Arzt, *Biochim. Biophys. Acta* **2000**, *1499*, 122–129.
[28] E. Stocklin, M. Wissler, F. Gouilleux, B. Groner, *Nature* **1996**, *383*, 726–728.
[29] M. Adams, O. C. Meijer, J. Wang, A. Bhargava, D. Pearce, *Mol. Endocrinol.* **2003**, *17*, 2583–2592.
[30] S. Lepine, J. C. Sulpice, F. Giraud, *Crit. Rev. Immunol.* **2005**, *25*, 263–288.
[31] L. R. Viegas, E. Hoijman, M. Beato, A. Pecci, *J. Steroid Biochem. Mol. Biol.* **2008**, *109*, 273–278.
[32] M. J. Herold, K. G. McPherson, H. M. Reichardt, *Cell. Mol. Life Sci.* **2006**, *63*, 60–72.
[33] H. M. Reichardt, K. H. Kaestner, J. Tuckermann, O. Kretz, O. Wessely, R. Bock, P. Gass, W. Schmid, P. Herrlich, P. Angel, G. Schutz, *Cell* **1998**, *93*, 531–541.
[34] G. Burton, C. P. Lantos, A. S. Veleiro, US Patent 7071328, **2006**.
[35] P. J. Godowski, S. Rusconi, R. Miesfeld, K. R. Yamamoto, *Nature* **1987**, *325*, 365–368.
[36] W. Kueng, E. Silber, U. Eppenberger, *Anal. Biochem.* **1989**, *182*, 16–19.
[37] Gaussian 03: M. J. Frisch, G. W. Trucks, H. B. Schlegel, G. E. Scuseria, M. A. Robb, J. R. Cheeseman, J. A. Montgomery, Jr., T. Vreven, K. N. Kudin, J. C. Burant, J. M. Millam, S. S. Iyengar, J. Tomasi, V. Barone, B. Mennucci, M. Cossi, G. Scalmani, N. Rega, G. A. Petersson, H. Nakatsuji, M. Hada, M. Ehara, K. Toyota, R. Fukuda, J. Hasegawa, M. Ishida, T. Naka-

jima, Y. Honda, O. Kitao, H. Nakai, M. Klene, X. Li, J. E. Knox, H. P. Hratchian, J. B. Cross, V. Bakken, C. Adamo, J. Jaramillo, R. Gomperts, R. E. Stratmann, O. Yazyev, A. J. Austin, R. Cammi, C. Pomelli, J. W. Ochterski, P. Y. Ayala, K. Morokuma, G. A. Voth, P. Salvador, J. J. Dannenberg, V. G. Zakrzewski, S. Dapprich, A. D. Daniels, M. C. Strain, O. Farkas, D. K. Malick, A. D. Rabuck, K. Raghavachari, J. B. Foresman, J. V. Ortiz, Q. Cui, A. G. Baboul, S. Clifford, J. Cioslowski, B. B. Stefanov, G. Liu, A. Liashenko, P. Piskorz, I. Komaromi, R. L. Martin, D. J. Fox, T. Keith, M. A. Al-Laham, C. Y. Peng, A. Nanayakkara, M. Challacombe, P. M. W. Gill, B. Johnson, W. Chen, M. W. Wong, C. Gonzalez, J. A. Pople, Gaussian Inc., Wallingford CT (USA), **2004**.

[38] D. A. Pearlman, D. A. Case, J. W. Caldwell, W. S. Ross, T. E. Cheatham III, S. DeBolt, D. Ferguson, G. Seibel, P. Kollman, *Comput. Phys. Commun.* **1995**, *91*, 1–41.

[39] R. K. Bledsoe, V. G. Montana, T. B. Stanley, C. J. Delves, C. J. Apolito, D. D. McKee, T. G. Consler, D. J. Parks, E. L. Stewart, T. M. Willson, M. H. Lambert, J. T. Moore, K. H. Pearce, H. E. Xu, *Cell* **2002**, *110*, 93–105.

[40] T. E. Cheatham III, P. Cieplak, P. A. Kollman, *J. Biomol. Struct. Dyn.* **1999**, *16*, 845–862.

[41] H. J. C. Berendsen, J. P. M. Postma, W. F. Van Gunsteren, A. DiNola, J. R. Haak, *J. Chem. Phys.* **1984**, *81*, 3684–3690.

Received: July 29, 2008
Revised: September 12, 2008
Published online on November 4, 2008

